Int. J. Heat Mass Transfer. Vol. 29, No. 12, pp. 1953–1961, 1986
Printed in Great Britain

0017–9310/86 $3.00 + 0.00
Pergamon Journals Ltd.

Role of macrolayer evaporation in pool boiling at high heat flux

A. M. BHAT,* J. S. SAINI†§ and R. PRAKASH‡

* Mechanical Engineering Department, Regional Engineering College, Srinagar, Jammu and Kashmir, India
† Alternate Hydro Energy Centre, University of Roorkee, Roorkee—247 667, India
‡ Mechanical and Industrial Engineering Department, University of Roorkee, Roorkee—247 667, India

(*Received* 18 *February* 1985 *and in final form* 18 *December* 1985)

Abstract—Analytical expressions for macrolayer thickness and the rate of heat transfer through a macrolayer in a high heat flux region near the critical value were reported in previous papers by the authors. The results of an experimental investigation into the liquid macrolayer formation are being reported in this paper. The initial thickness of this liquid layer formed between the heated surface and the vapour mass and the frequency of the vapour mass as a function of impressed heat flux have been measured. Using these data, the contribution of macrolayer evaporation to the heat flow from heated surface to bulk has been estimated. Experimental results of macrolayer thickness and frequency of vapour mass have been found to compare well with analytically predicted values. Contribution of heat conduction through the macrolayer has also been found to account for a considerable portion of wall heat flux.

INTRODUCTION

IT IS well known that in pool boiling the high heat flux region near the critical value is characterized by the formation of a thin liquid layer beneath a growing vapour mass [1–3]. This liquid layer is known as the macrolayer. Based on the analysis of the mechanism of formation of the macrolayer, an expression for initial macrolayer thickness (at the instant of its formation) was derived [3]. It was hypothesized [4] that the heat transfer in this region takes place mainly due to heat conduction through the liquid macrolayer, resulting in vapour mass growth and subsequent departure. In this paper the experimental results obtained by the authors are presented and compared with those obtained from the analysis.

EXPERIMENTAL WORK

An experimental apparatus was fabricated to obtain pool boiling data at atmospheric pressure in the entire regime of pool boiling up to critical heat flux. Figure 1 is a diagram of the experimental apparatus. The major components of the apparatus are the heater assembly, boiler vessel, condenser assembly, electrical resistance probe, three-dimensional microtraveller and a high speed camera. The heater, boiler and condenser assembly are very similar to those used by Gaertner [1]. Heat generation took place in a solid copper block (155 mm diameter and 205 mm long), through nine 600-W heater rods inserted in holes drilled in the copper block and insulated with 3-mm-thick porcelain powder rammed into the annular space between the heater rod and the copper block. A 70-mm-long, 42-mm-diameter copper rod was placed in a cup-shaped cavity made in the copper block and separated by a thin layer of tin–lead solder alloy which would be in a molten state at the operating temperatures, thus reducing thermal resistance between the two mating surfaces because the presence of liquid layer will provide better contact and nearly complete expulsion of air. The top surface of this copper rod, which served as the boiling surface, was polished to 4/0 emery grade. A pair of mating Teflon rings, one fitted on the top of the copper conductor and the other riveted on the stainless-steel fin (Fig. 1), made the assembly leak-proof and provided good insulation at the top of the copper conductor. Six calibrated chromel–constantan thermocouples were mounted on the heater rod to monitor the temperature of the boiling surface and the temperature gradient in the heater. The temperature profile was extrapolated to the heater surface to find its surface temperature and the wall temperature gradient. The extrapolation was made possible by the linear profile experimentally obtained. The boiler vessel (150 mm diameter and 400 mm long) was made from 304-stainless-steel sheet. The heater assembly could be detached from the boiler vessel and brought down to a lower position to enable the boiling surface to be cleaned and polished for each run. Distilled water was used as the boiling fluid. The condensate was preheated to saturation temperature before flowing to the boiler vessel. A guard heater mounted on the boiler vessel maintained the fluid at saturation temperature.

The electrical resistance probe technique [5] was used to measure the bubble emission frequency and the macrolayer thickness. The detecting part consists of an insulated probe with an exposed tiny electrode projecting into the fluid; the other electrode is the boiling surface which is assumed to be always in contact with the liquid. The electrical resistance between

§ To whom correspondence should be addressed.

NOMENCLATURE

C	specific heat of liquid [J kg^{-1} K^{-1}]	q_w	wall heat flux [W m^{-2}]
D_d	bubble departure diameter [m]	t_g	growth period [s]
f	bubble departure frequency [Hz]	ΔT	temperature difference [K]
F	vapour mass frequency [Hz]	$\bar{u}$	average bubble rise velocity [m s^{-1}].
h	heat transfer coefficient [W m^{-2} K^{-1}]		
h_{fg}	latent heat of vaporization [J kg^{-1}]		
h_{nc}	heat transfer coefficient due to natural convection [W m^{-2} K^{-1}]	Greek symbols	
		δ_0	macrolayer thickness [m]
h_{nuc}	heat transfer coefficient due to nucleation [W m^{-2} K^{-1}]	θ_0	degree of superheat [K]
		ρ	density of liquid [kg m^{-3}]
k	thermal conductivity [W m^{-1} K^{-1}]	ρ_v	density of vapour [kg m^{-3}]
N/A	density of active sites [m^{-2}]	α	thermal diffusivity [m^2 s^{-1}].

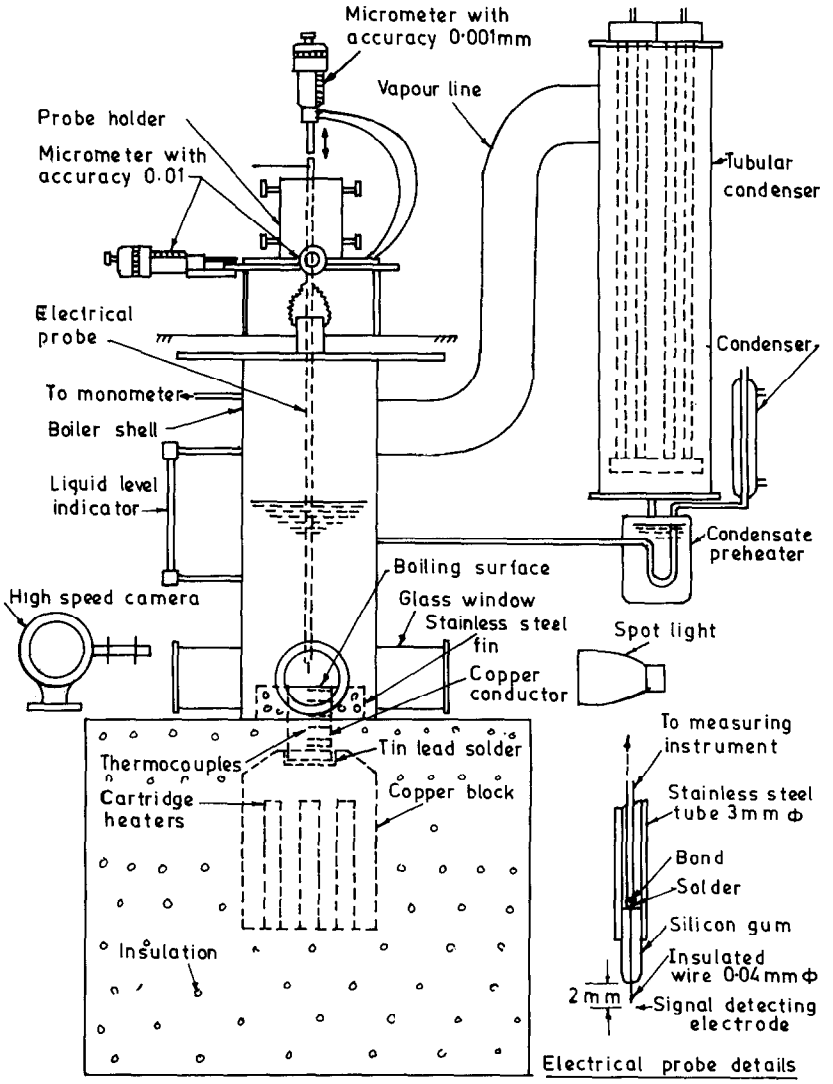

FIG. 1. Sketch of experimental apparatus.

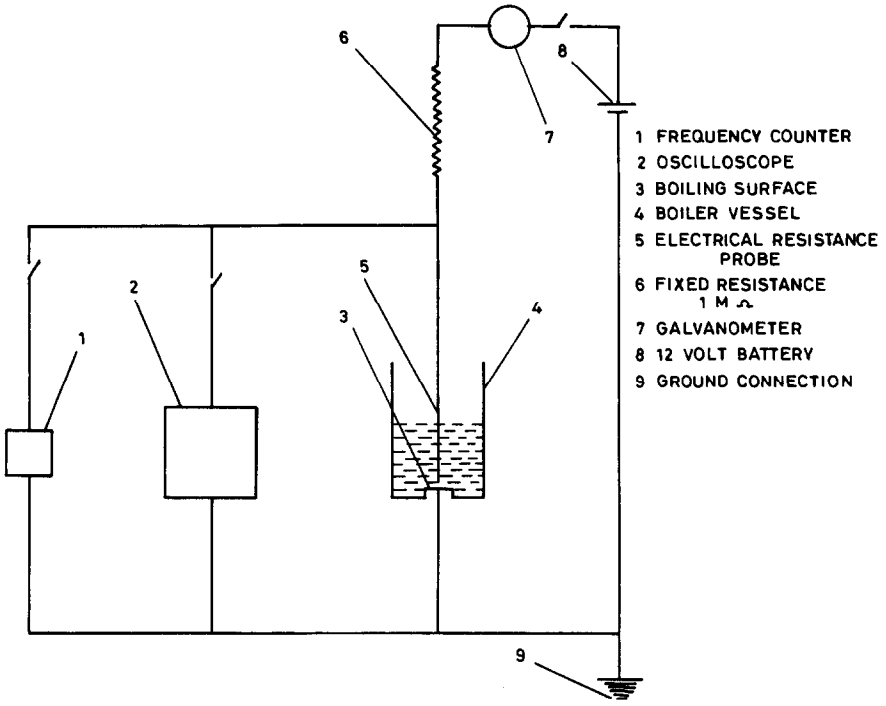

FIG. 2. Circuit diagram for frequency measurement.

these two electrodes is a function of the state of the matter in contact with the probe. Figure 2 shows the circuit diagram for the measurement of vapour mass or bubble frequency. The probe was energized with a 12 V d.c. electric supply through a fixed resistance. With the probe tip just above an active site, a square wave of the form shown in Fig. 3 was observed. A digital frequency counter was used to record the frequency. The sensitivity and the calibration of the frequency counter were checked with an oscillator. A number of oscilloscope traces were photographed with an oscilloscope camera. The calibration of the frequency counter was also checked with the frequency obtained from the photographs of the traces. The frequency counter was found to be sensitive to voltage signals greater than 0.3 V. The supply voltage and the fixed resistor were so chosen that the signal obtained was of about 0.7 V amplitude when the probe tip was in vapour. The ripples observed on the oscilloscope trace were of much lower amplitude and hence could be assumed to have no effect on the reading from the frequency counter.

A three-dimensional microtraveller was used to provide accurately controlled micro-displacements to the probe in the vertical as well as two perpendicular, horizontal directions. The high speed motion pictures were taken at 500 f.p.s. using a HYSPEED camera. Timing marks on the film were provided by a 100 Hz timing light generator. Three 1000-W incandescent lights one at each of the three glass windows provided the illumination on the boiling surface.

FIG. 3. Square wave as seen on the oscilloscope. Each cycle corresponds to one cycle of bubble formation.

It was found that if the power input to the copper block was increased through large steps, film boiling could occur prematurely. Due to this, high heat flux values were approached by increasing power input slowly and gradually. A number of runs were repeated to check the reproducibility which was found to be satisfactory. On attaining steady state, the liquid was permitted to boil for about 2 h before recording the data. The high thermal capacity of the copper block saved the equipment from overheating and burning out. The only damage that occurred during the film boiling was overheating of the Teflon ring in contact with the copper conductor which had to be replaced.

MEASUREMENT OF FREQUENCY AND MACROLAYER THICKNESS

While recording the bubble or vapour mass frequency at a particular site, the probe tip was brought to about 3 mm above the heating surface and then slowly pushed down by means of a vertical micrometer through known micro-displacements and at each position, the frequency was recorded. The process was repeated until the probe tip touched the heating surface. The physical contact of the probe tip with the surface was marked by an impulse of high current flow through the galvanometer in the circuit. Figure 4 shows a typical curve of the frequency vs

height at heat flux of 0.157×10^6 W m^{-2}. Isolated bubbles were observed at random active sites at this heat flux and the probe was visually positioned over an active site. It is seen that the frequency increases from A to B, remains fairly constant from B to C and decreases slightly beyond C downwards until the probe touches the heating surface. The frequency values between B and C appear to be the frequencies of the individual vapour bubbles departing from the heating surface. The drop in frequency above B may be due to deviation of paths of some of the bubbles where a decrease below C may be attributed to interference of the probe with bubble formation phenomenon when the probe is very close to the heating surface. At each heat flux value, the frequency measurements were made at a number of locations in the horizontal plane.

Because of the high active site density at high heat flux and the highly transient nature of the phenomenon, direct measurement of the macrolayer is not feasible. In this work the values of the macrolayer thickness were obtained in an indirect manner, from the plots of frequency. A typical frequency curve at a heat flux of 0.988×10^6 W m^{-2} is shown in Fig. 5. It appears that at a height of about 3 mm, the probe was initially in the vapour mass. As the probe is pushed closer to the heating surface, the frequency increases till it attains a maximum value at B. Further downward movement of the probe indicates a drop in frequency to a very low value. It is assumed that the increase in frequency between points A and B is caused by individual bubbles which are formed at active sites and merge with the vapour mass which has already been detached. The sudden decrease in frequency at point B indicates that the probe is in a liquid-rich layer in the region. Oscilloscope traces support this view since at a point below B the period for which the probe remained in liquid was observed to be much higher compared to that observed above point B. The height of point B above the heating surface could therefore be reasonably assumed to be the initial macrolayer thickness. The fall in frequency below B appears to be due to interference of the probe with the bubble growth process. In the high heat flux region, the bubble departure diameter is of the order of 0.1 mm whereas the probe has an outer diameter of 0.06 mm including its insulation. The copper probe wire being very close to the heated surface could conduct heat from the superheated liquid in the macrolayer. This heat loss near an active site could cause local suppression of nucleation of the affected site. In the low heat flux region the suppression effect was comparatively insignificant because of lower active site density and larger bubble departure diameter and hence the area affected was only a small percentage of the total.

VAPOUR MASS FREQUENCY

High speed photographs were used to determine the value of the frequency of the vapour mass. These values were found to be close to those obtained by electrical probes. Figure 6 shows sample photographs at various heat fluxes. The scale of those photographs is 0.183 times actual size. Growth of the vapour mass is represented by an increase in the height of the shaded image. The shade is caused by the reflection of light by the vapour mass which differentiates it from the liquid region above the vapour mass. Isolated bubbles seen in the photographs appear to have been formed on the peripheral portion of the heating surface. The photograph corresponding to low heat flux shows no vapour mass but only isolated bubbles. The frequency of the vapour mass was obtained from the time interval between departure of two successive vapour masses. For each run, the frequency was determined for the number of cycles and an average value obtained.

RESULTS AND DISCUSSION

The equation proposed for initial macrolayer thickness [3] was

$$\delta_0 = \frac{D_d}{2} + \bar{u}(x^2 - t_g) \tag{1}$$

where

$$x = \tfrac{1}{2}[-(1/k_1) + (1/k_1^2 + 4k_2)^{1/2}]$$

$$k_1 = \bar{u}(fD_d/\bar{u} - 1)/(8M\theta_0)$$

$$K_2 = [(D_0 - D_d)/(4M\theta_0) + t_g^{1/2} + k_1 t_g]/k_1$$

$$M = \rho C\sqrt{\alpha}/(\sqrt{\pi}\rho_v h_{fg})$$

$$D_0 = (A/N)^{1/2}.$$

Figure 7 shows the comparison of the experimental results and the analytical results of equation (1). In order to carry out the analytical calculation of the value of macrolayer thickness, the following relations were used in conjunction with equation (1) [5]

$$fD_d = 111 \text{ m s}^{-1} \text{ [6]}$$

$$N/A = (h - h_{nc})/[\pi D_d^2 (h_{nuc} - h_{nc})] \text{ [7]}$$

$$h_{nc} = 0.15[g\beta C\rho^2 k^2/\mu]^{1/3} (\Delta T)^{1/3}$$

$$h_{nc} = 2(\rho Ck)^{1/2} f^{1/2}/\sqrt{\pi}.$$

It is seen from Fig. 7 that the predicted values of macrolayer thickness are in good agreement with the experimental values.

A best fit curve into the experimental data has been found to be

$$\delta_0 = 1.585 \times 10^5 q_w^{-1.527}. \tag{2}$$

Equation (2) is comparable with the results of Gaertner [1]

$$\delta_0 = 0.4854 \times 10^5 q_w^{-1.4225} \tag{3}$$

and Iida and Kobayasi [2]

$$\delta_0 = 3.2296 \times 10^5 q_w^{-1.5148}. \tag{4}$$

Equations (3) and (4) have also been plotted along with (1) and (2) in Fig. 8.

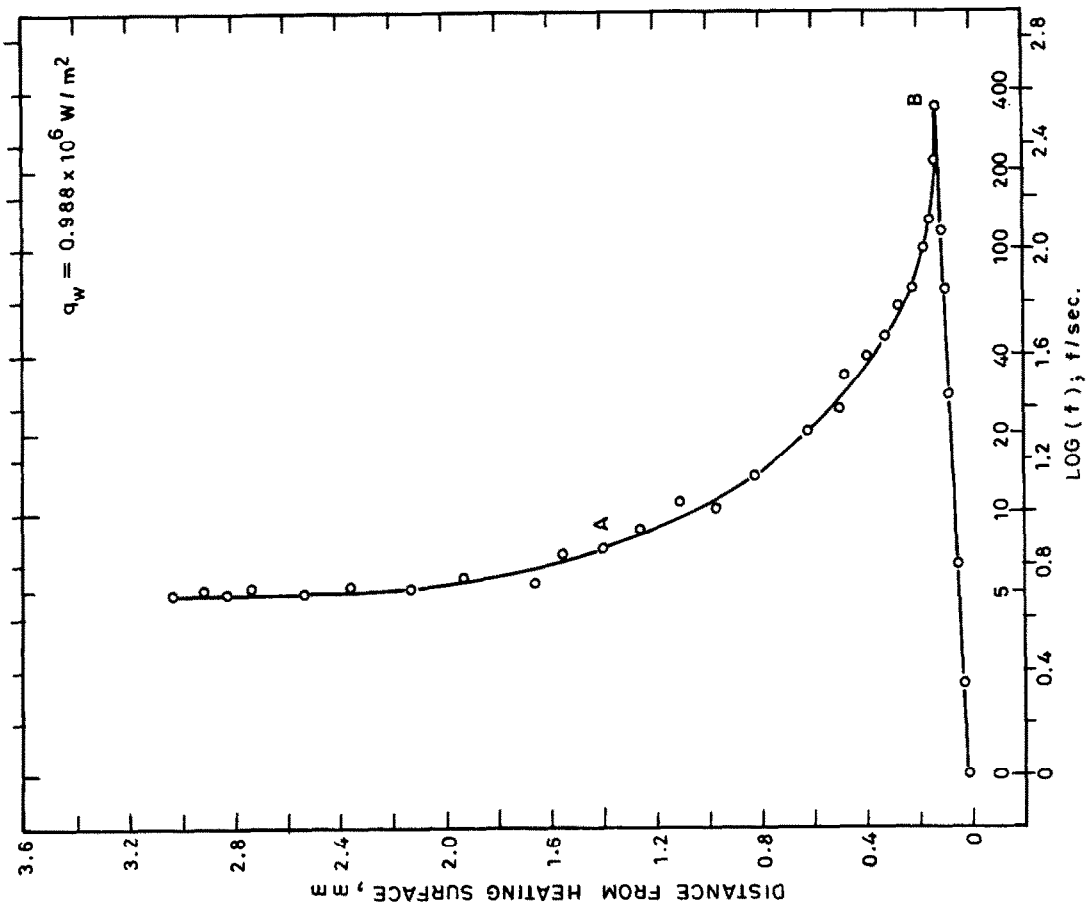

FIG. 5. Experimental frequency record at different locations above the heated surface.

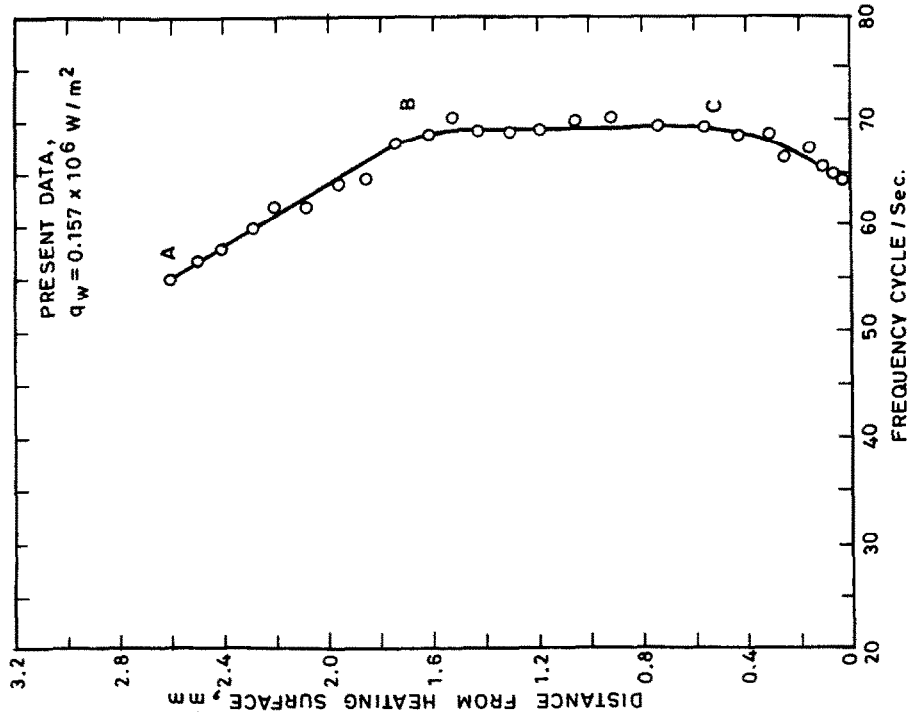

FIG. 4. Experimental frequency record at different positions of the probe above the heated surface.

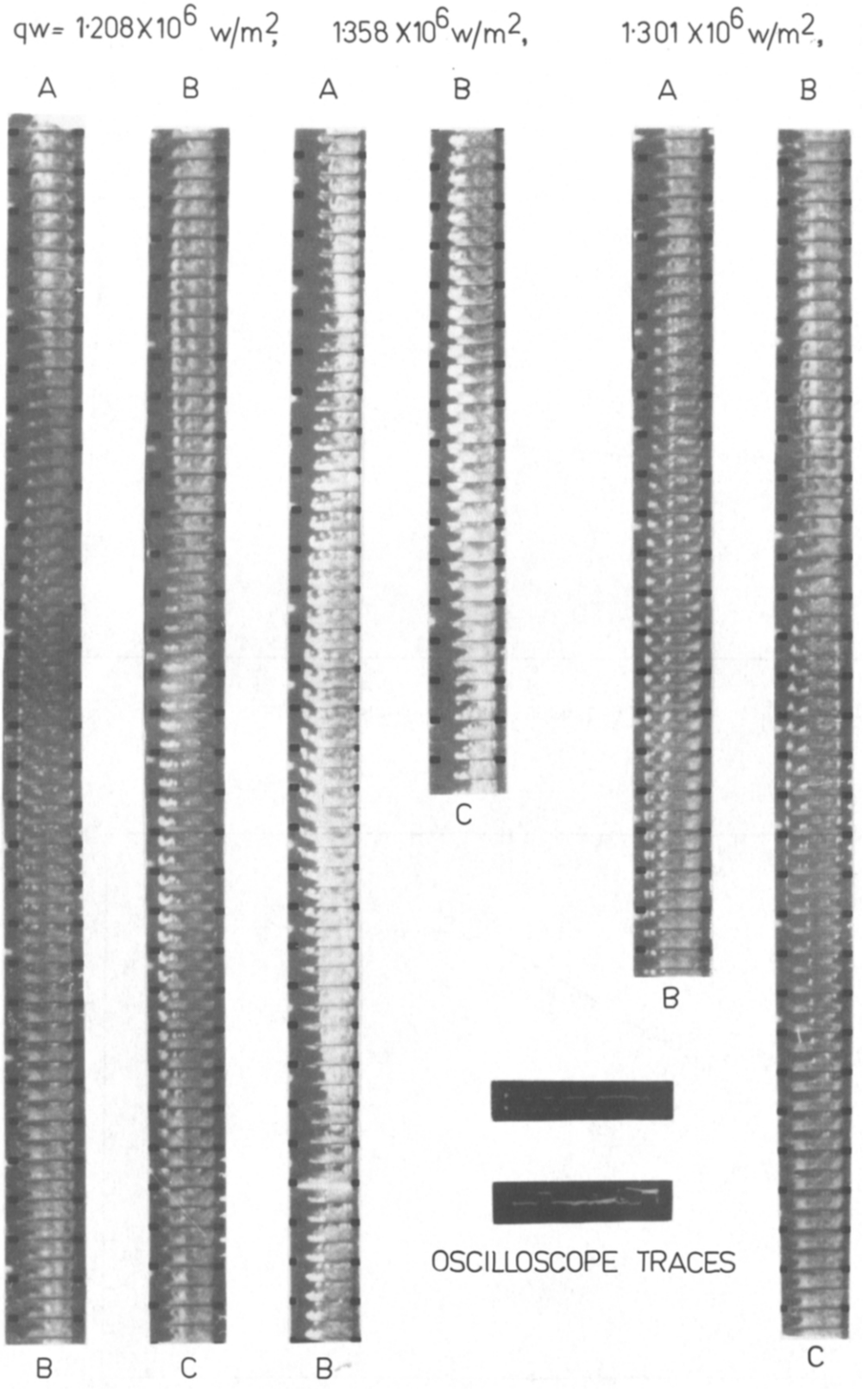

FIG. 6. High speed photograph sequences.

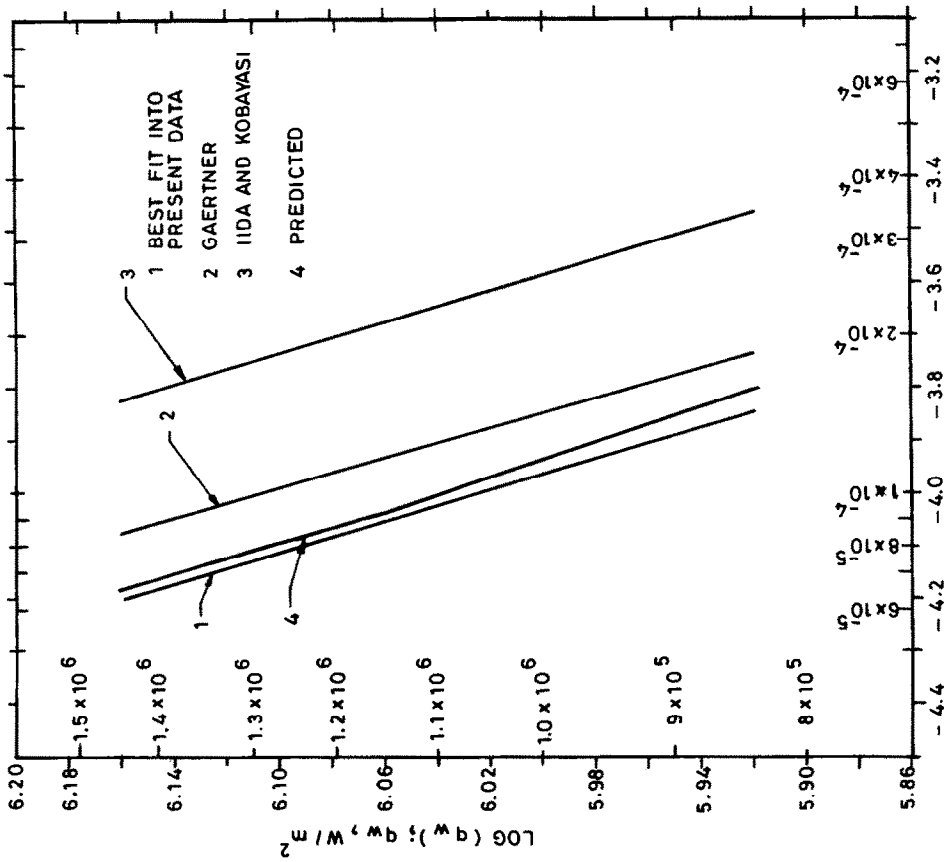

FIG. 8. Data on δ_0 vs q_w of Gaertner [1], Iida and Kobayasi [2] and present work (best fit curves) compared with the theoretical results.

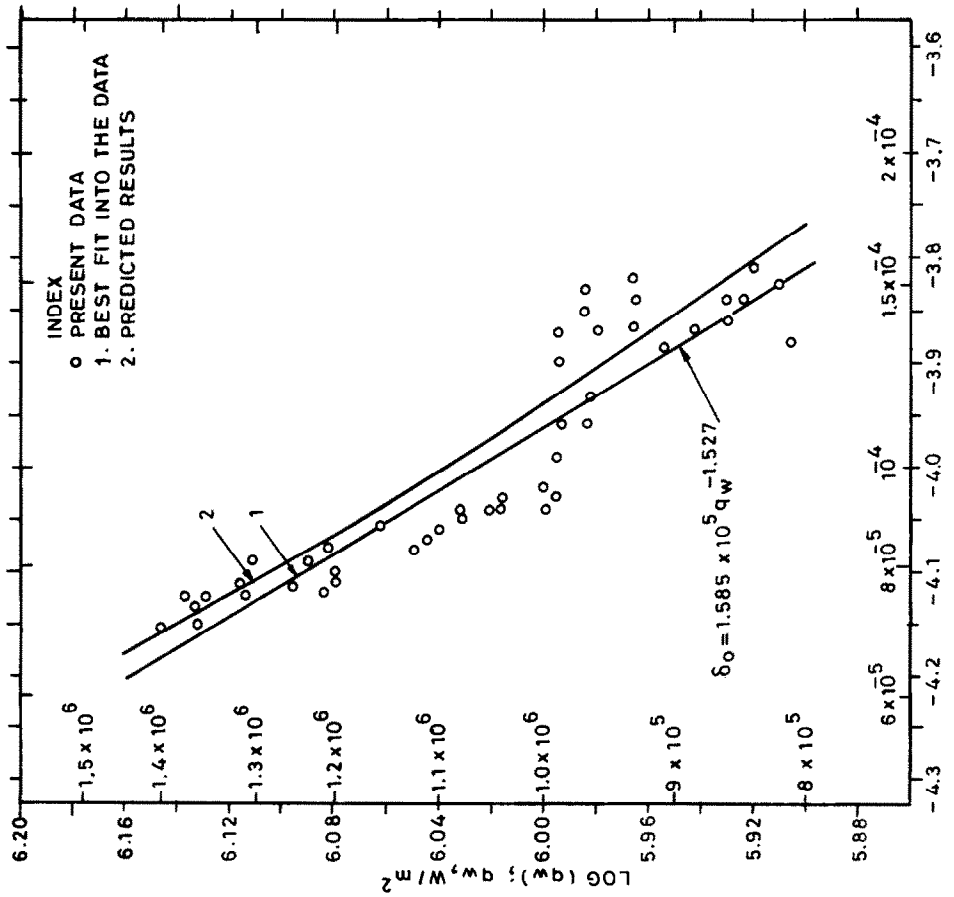

FIG. 7. Experimental and predicted initial macrolayer thickness vs heat flux.

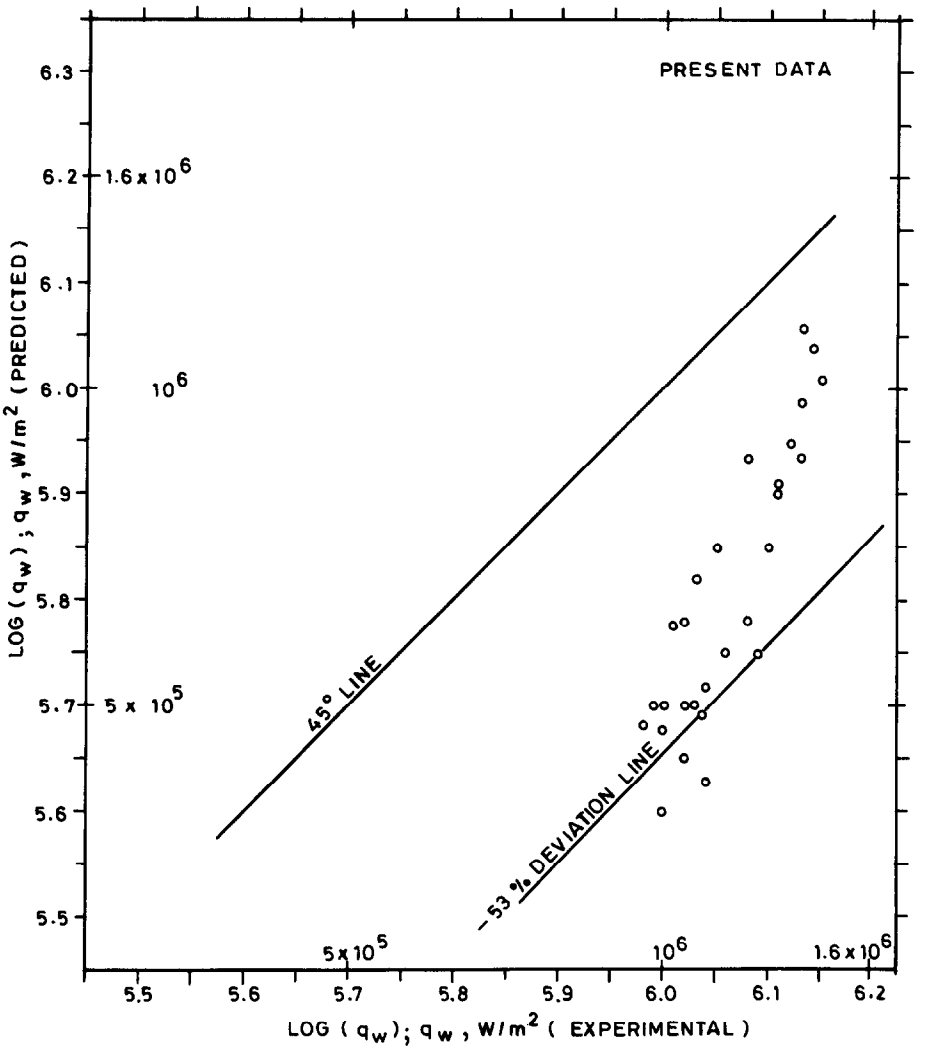

FIG. 9. Comparison of experimental wall heat flux with corresponding predicted values.

A best fit curve into the experimental data of vapour mass frequency has been found to be

$$F = 1.595 \times 10^{-10} q_w^{-1.576}. \quad (5)$$

Conduction heat flux through the macrolayer has been found to be [5]

$$\bar{q}_{cond} = \frac{\rho h_{fg} k \Delta T F}{q_w} \ln\left[\frac{\delta_0}{\delta_0 - q_w/(\rho h_{fg} F)}\right]. \quad (6)$$

Experimental values of wall heat flux, q_w, wall superheat, ΔT, and the vapour mass frequency, F, have been used to calculate the average conduction heat flux, $\bar{q}_{cond}$, from equation (6). Figure 9 compares the experimental heat flux values (q_w) with the calculated values of average conduction heat flux ($\bar{q}_{cond}$). A reasonably good agreement has been found; the deviation decreasing with increase in heat flux indicating that the contribution of heat conduction through the macrolayer is higher at high heat flux conditions. These results show that the heat transfer model assuming conduction across the liquid macrolayer formed under the vapour mass can account for the major portion of heat transfer from heating surface in the high heat flux region of pool boiling.

CONCLUSION

The contribution of heat conduction through the macrolayer accounts for a major portion of heat flow in the high heat flux region in pool boiling; the contribution decreases with decrease in heat flux.

REFERENCES

1. R. F. Gaertner, Photographic study of nucleate pool boiling on a horizontal surface, *J. Heat Transfer* **87C**, 17 (1965).
2. Y. Iida and K. Kobayasi, Distribution of void fraction above a horizontal heating surface in pool boiling, *Bull. J.S.M.E.* **12**, 283 (1969).
3. A. M. Bhat, R. Prakash and J. S. Saini, On the mechanism of macrolayer formation in nucleate pool boiling at high heat flux, *Int. J. Heat Mass Transfer* **26**, 735–740 (1983).

4. A. M. Bhat, R. Prakash and J. S. Saini, Heat transfer in nucleate pool boiling at high heat flux, *Int. J. Heat Mass Transfer* **26,** 833–840 (1983).
5. A. M. Bhat, Studies on bubble dynamics and heat transfer in nucleate pool boiling at high heat flux. Ph.D. thesis, Department of Industrial Engineering, University of Roorkee, Roorkee, India (1982).
6. K. Nishikawa and Y. Fujita, Correlation of nucleate pool boiling heat transfer based on bubble population density, *Int. J. Heat Mass Transfer* **20,** 233 (1977).
7. K. Bier, D. Goneflo, M. Salem and Y. Tanes, Pool boiling heat transfer and size of active nucleation cavities for horizontal plates with different surface roughnesses, *Proc. 6th Int. Heat Transfer Conference*, Vol. 1, p. 151 (1978).

ROLE DE L'EVAPORATION EN MACROCOUCHE DANS L'EBULLITION EN RESERVOIR A HAUT FLUX DE CHALEUR

Résumé—Des expressions analytiques pour l'épaisseur de la macrocouche et le flux de chaleur à travers une macrocouche dans le domaine de grand flux de chaleur, près de la valeur critique, sont données par les auteurs dans des articles antérieurs. Les résultats d'une étude expérimentale sur la formation de la macrocouche liquide sont reportés ici. On a mesuré l'épaisseur initiale de cette couche formée entre la surface chaude et la masse de vapeur et la fréquence de la masse de vapeur en fonction du flux de chaleur imposé. A partir de ces données, la contribution de l'évaporation en macrocouche au flux de chaleur transféré depuis la surface est estimée. Les résultats expérimentaux se comparent bien avec les valeurs calculées. La contribution de la conduction de chaleur à travers la macrocouche est trouvée compter pour beaucoup dans le flux de chaleur pariétal.

DIE ROLLE DER MAKROSCHICHTVERDAMPFUNG BEIM BEHÄLTERSIEDEN MIT HOHEN WÄRMESTROMDICHTEN

Zusammenfassung—In früheren Veröffentlichungen der Autoren wurden analytische Ausdrücke für die Dicke der Makroschicht und den Wärmestrom durch die Makroschicht im Bereich hoher Wärmestromdichten nahe dem kritischen Wert mitgeteilt. In dieser Arbeit werden Ergebnisse einer experimentellen Untersuchung zur Bildung der Flüssigkeits-Makroschicht vorgestellt. Die ursprüngliche Dicke der Flüssigkeitsschicht zwischen der beheizten Oberfläche und der Dampfmenge und die Frequenz der Dampfmenge als Funktion der aufgeprägten Wärmestromdichte wurden gemessen. Anhand dieser Daten wurde der Beitrag der Makroschichtverdampfung am Wärmestrom von der beheizten Oberfläche an das umgebende Fluid ermittelt. Die experimentellen Ergebnisse der Makroschichtdicke und der Frequenz der Dampfmenge stimmten gut mit den analytisch berechneten Werten überein. Die Wärmeleitung durch die Makroschicht überträgt ebenso einen erheblichen Teil des gesamten Wärmestroms.

РОЛЬ ИСПАРЕНИЯ МАКРОСЛОЯ ПРИ КИПЕНИИ В БОЛЬШОМ ОБЪЕМЕ ПРИ БОЛЬШИХ ТЕПЛОВЫХ ПОТОКАХ

Аннотация—В предыдущей работе авторами даны аналитические выражения для толщины макрослоя и интенсивности теплопереноса через макрослой при высоких тепловых потоках вблизи критического значения. Представлены результаты экспериментального исследования образования макрослоя жидкости. Измерены начальная толщина слоя жидкости, образованного между нагретой поверхностью и массой пара, и скорость образования пара как функция внешнего теплового потока. С использованием этих результатов оценен вклад испарения макрослоя в тепловой поток со стороны нагретой поверхности в большой объем. Найдено хорошее соответствие данных экспериментов по толщине макрослоя и скорости образования пара с результатами аналитических расчетов. Вклад теплопроводности через макрослой составляет значительную часть теплового потока от стенки.